A complete photometric study of the open cluster NGC 7790 containing Cepheid variables[⋆]

A.C. Gupta[1,2,3]**, A. Subramaniam**[3]**, R. Sagar**[2,3]**, and W.K. Griffiths**[4]

[1] Department of Physics, University of Gorakhpur, Gorakhpur 273 009, India
e-mail: acgupta@prl.ernet.in
[2] U.P. State Observatory, Manora Peak, Naini Tal 263 129, India
[3] Indian Institute of Astrophysics, Bangalore 560034, India
[4] Department of Physics, University of Leeds, Leeds LS2 9JT, UK

Abstract. CCD photometry of the northern open star cluster NGC 7790 has been carried out in BVI photometric passbands down to $V \sim 21$ mag for 1150 stars of which for ~ 700 stars, the data is obtained for the first time. We derive the most reliable parameters for this cluster using all the available photometric, spectroscopic and proper motion data. The interstellar extinction over the cluster area is uniform and normal with $E(B-V) = 0.51 \pm 0.03$ mag. We determine a distance of 3.3 ± 0.23 Kpc to the cluster. The theoretical isochrone fittings to the Cepheid variables as well as the evolved part of the main-sequence near turn-off point indicate that the cluster is 120 ± 20 Myr old. We estimate the cluster radius to be $3.\!'7$ using radial stellar density profile. Both the distance and age determined using period luminosity/age relations for the Cepheid variables are consistent with their membership of the cluster. This unique opportunity has therefore been used to refine the zero-point of the period-luminosity relation for the Galactic Cepheids.

Key words: Galaxy: open clusters: individual: NGC 7790 — stars: evolution — HR diagram

1. Introduction

The colour-magnitude diagram (CMD) of a star cluster is an important tool to obtain the information on distance and age of the cluster and interstellar extinction in the direction of cluster. Accurate deep photometric observations down to $V > 20$ mag are necessary for such studies and the same is presented here for NGC 7790.

The northern galactic open cluster NGC 7790 = C2355 + 609 ($l = 116°\!.6, b = -1°\!.0$) is near the Perseus spiral arm. It has been classified as Trumpler Class II2m by Lyngå (1987) and as an intermediate age star cluster by Mermilliod (1981). The cluster radius is $2.\!'5$ and it has the unique characteristic of containing three Cepheids namely CEa Cas, CEb Cas and CF Cas (see Kraft 1958; Sandage 1958; Schmidt 1981; Pedreros et al. 1984). UBV photoelectric photometry of 33 stars and photographic photometry of 100 stars were obtained by Sandage (1958). He estimated the distance of the cluster to be 3630 ± 250 pc. Pedreros et al. (1984) carried out UBV photographic photometry down to $V \sim 19$ mag and derived a mean value of $E(B-V) = 0.64 \pm 0.05$ mag and a true distance modulus of $(m-M)_0 = 12.3 \pm 0.2$ mag. Romeo et al. (1989) obtained $BVRI$ CCD photometry and they derived the value of $E(B-V) = 0.54 \pm 0.04$ mag; $(m-M)_0 = 12.65 \pm 0.15$ mag and age of 50 ± 15 Myr using classical models and 100 ± 20 Myr adopting models with overshooting of the convective core. Iyeshima et al. (1994) obtained BVR CCD photometric observations, while Phelps & Janes (1994) obtained UBV CCD data for this cluster. Frolov (1977) determined relative proper motions of stars of the cluster region in an area of $1° \times 1°$ with the center at $\alpha = 23^{\mathrm{h}}54^{\mathrm{m}}12^{\mathrm{s}}, \delta = +60°57'$ (1950.0) and found 60 stars to be members of NGC 7790 down to a limiting magnitude $B = 16.5$ mag. Membership probabilities were also computed by Zhao et al. (1984) using the proper motion measurements given by Ishmukamedov (1966). However, due to relatively large distance of the cluster combined with the limited precision of the data, these proper motion data are not very useful to separate cluster members from the field-stars.
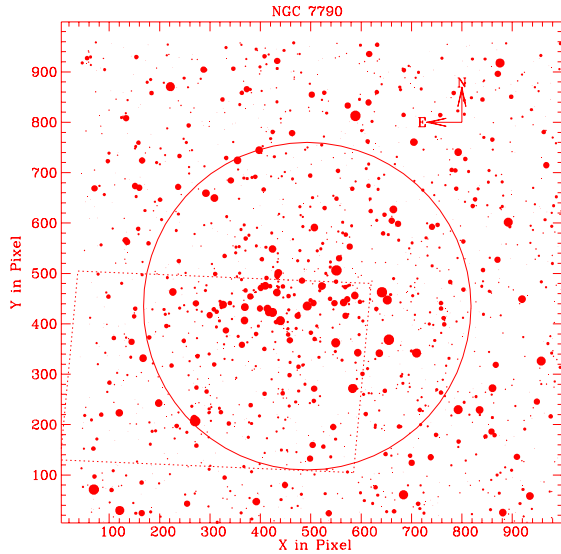
[⋆] Table 1 is only available in electronic form at the CDS via anonymous ftp to cdsarc.u-strasbg.fr (130.79.128.5) or via http://cdsweb.u-strasbg.fr/Abstract.html

Fig. 1. Identification map of the NGC 7790 region. The (X, Y) coordinates are in pixel units and one pixel corresponds to $0''.74$ on the sky. North and East directions are marked. Filled circles of 9 sizes (each corresponding to one magnitude range in V) are used to represent brightness of the stars. Largest and smallest sizes denote stars in the brightest and faintest magnitude range of $V = 11$ to 12 and 19 to 20 respectively. Open circle denotes the cluster radius of $3'.7$ with Sandage (1958) star E at the center. The region imaged by us is shown by dotted line

In spite of a number of photoelectric, photographic and CCD photometric studies of the cluster, its parameters are not well determined as they have a range of values, e.g. $E(B - V) = 0.5$ to 0.7 mag and distance $= 2.4$ to 3.6 Kpc (see Tables 2 and 3 in Romeo et al. 1989). In this paper we present a new deep BVI CCD photometric observations of the stars in the field of NGC 7790 and use them along with existing photometric, spectroscopic, proper motion and Space Telescope Science Institute digitized sky survey (DSS) data to derive the best determinations of radius, distance, interstellar extinction and age of the cluster NGC 7790 which in turn allow a more precise determination of the fundamental parameters of the Cepheids such as the zero-point of the period luminosity/age relations.

The observations, data reductions and comparison of various photometries are given in the next two sections. The field-star contamination, interstellar extinction, other photometric results and their implications for the membership of the Cepheids are described in the subsequent sections of this paper.

2. Observations and data reductions

The observations of NGC 7790 were carried out in B, V Johnson and I Cousins passbands using RCA SID 501 thinned back illuminated CCD detector at the $f/3.29$ Prime focus of the 2.3 meter Issac Newton Telescope (INT) at La Palma. At the Prime focus, a pixel of

the 320×512 size CCD corresponds to $0''.74$. Bias and dark frames were taken intermittantly. Flat-field exposures ranging from 1 to 10 seconds in each filter were made of the twilight sky. Nine Landolt (1983) standards, covering a range in brightness $(10 < V < 13)$ as well as in colour $(-0.19 < (V - I) < 1.41)$ were observed for calibration purpose. The region as shown in Fig. 1, was imaged on the nights of 1988 July 21 and 22. Altogether 9, 8 and 8 frames were taken in B, V and I passbands respectively. The exposure times were 50, 40 and 40 seconds in the respective passbands. Further details of the instrument and observing procedures have been given in Sagar & Griffiths (1991).

Initial processing of the data frames as well as photometric reductions were carried out at Indian Institute of Astrophysics, Bangalore. The evenness of flat-field frames (summed for each colour band) is better than a few percent in all the filters. The magnitude estimation on each frame has been done using DAOPHOT profile fitting software (Stetson 1987, 1992). The stellar point spread function (PSF) was evaluated from several uncontaminated stars present in each frame. The image parameters and errors provided by DAOPHOT were used to reject poor measurements. About 10% stars were rejected in this process. DAOMASTER programme was used for cross identifying the stars measured on different frames of the cluster region.

The values of atmospheric extinction coefficients in the V passband determined during the observations by the Carlsberg Automatic meridian circle were between 0.10 and 0.11 mag per unit air mass with almost negligible $(\sim -0.003 \text{ mag})$ hourly rate of change of extinction. These along with mean $(B - V)$ atmospheric extinction coefficients for the site were used in determining the colour equations for the CCD system using Landolt (1983) standards (see Sagar & Griffiths 1991). In order to convert accurately the CCD instrumental magnitudes into standard ones using this colour equations, precise knowledge of the zero-points is required. It can be achieved if standards in the imaged regions are present, as it avoids the errors introduced due to uncertainties in shutter timing and in correction between profile and aperture magnitudes etc. Fortunately, such standard stars are present in the imaged cluster region and their CCD photometric measurements have been carried out earlier by Christian et al. (1985) and recently by Odewahn et al. (1992). The two sets of measurements agree very well with each other. Zero-points for the calibration have therefore been determined from the Christian et al. (1985) standards. The zero-points thus derived are uncertain by ~ 0.01 mag in B, V and I bands. The X and Y pixel coordinates as well as $V, (B - V)$ and $(V - I)$ magnitudes of the stars observed in NGC 7790 are listed in Table 1, which is available only in electronic form at the CDS in Strasbourgh and the open cluster database Web site at http://obswww.unige.ch/webda/. In order to avoid introductions of a new numbering and (X, Y)

Table 2. Internal photometric errors as a function of brightness in NGC 7790 are tabulated. The standard deviation (σ) is per observation in magnitudes

Magnitude Range	σ_B	σ_V	σ_I
$15.0 - 16.0$	0.01	0.01	0.03
$16.0 - 17.0$	0.05	0.08	0.04
$17.0 - 18.0$	0.09	0.11	0.08
$18.0 - 19.0$	0.12	0.15	0.11
$19.0 - 20.0$	0.14	0.17	0.18
$20.0 - 21.0$	0.25	0.29	0.26

coordinate systems, we adopt them from the database given by Phelps & Janes (1994). Stars not observed earlier have number starting with 5000 and there are about 700 such stars. They are mostly fainter than $V = 19$ mag, as present photometric data are the deepest. Stars observed by others have been identified in the last column of Table 1. The internal errors as a function of brightness for each filter are estimated using artificial add-star experiment as described by Stetson (1987) and they are given in Table 2. The errors become large (≥ 0.2 mag) for stars fainter than $V = 20$ mag, so the measurements should be considered unreliable below this magnitude.

2.1. Colour magnitude diagrams based on present observations

The apparent $V, (B - V)$ and $V, (V - I)$ diagrams of NGC 7790 generated from the present data are displayed in Fig. 2. These include all the stars with DAOPHOT $\sigma_{B-V}, \sigma_{V-I} < 0.07$. The deep CMDs extend down to $V = 20$ mag. A well defined cluster main-sequence (MS) contaminated by field-stars is clearly visible in both CMDs. The cluster sequences fainter than $V = 20$ have large scatter and perhaps not clearly defined. This may be due to large photometric errors present in our observations. In order to derive the most reliable cluster parameters, present data are not adequate as it covers only part of the cluster region (see Fig. 1) and also the cluster members brighter than $V = 13.5$ mag have not been observed. These stars are very important for estimating the cluster age and also for the study of stellar evolutionary status of the cluster. We have therefore combined all the broad band photometric data of the cluster available in the literature. For this, their inter-comparison is mandatory and the same has been done in the next section.

3. Comparison of various photometries

In order to provide the best set of $UBVRI$ magnitudes for the stars in the cluster region, we inter-compare the present CCD photometry and the earlier photoelectric, photographic and CCD photometric observations. For this, we used the open cluster database compiled by Mermilliod (1995). This database cross identifies the stars among the available observations with respect to the star number given by Phleps & Janes (1994). We also have therefore cross identified the stars common between present and Phleps & Janes (1994) measurements. For photometric comparison, only those sources in the cluster database are used where number of observed stars is at least 10. There are four such sources with UBV photoelectric data; one with UBV CCD data; two with BVR CCD data; one with I CCD data and three with UBV photographic data. The differences (Δ) between the various data sets are plotted in Fig. 3 and the statistical results are listed in Table 3. These show that in CCD observations, the distribution of the photometric differences seems fairly random with a constant zero-point offset, except for a few outliers, which appear to be mostly stars that were treated as single in one CCD study and as blended doubles in others. As expected, the scatter increases with decreasing brightness and becomes more than ~ 0.1 mag at fainter levels. Considering these and the uncertainties present in photometric measurements, we conclude that,

(i) in general UBV photoelectric data are in fairly good agreement with the CCD data. Except for a few outliers, the distribution seems to be fairly random with a constant zero offset but no dependence on brightness;

(ii) the photographic data show systematically increasing or decreasing differences with the CCD data in all magnitudes. The scatter is larger in comparison to the photoelectric and CCD data. The difference in V increases with faintness and become ~ 0.2 mag at $V \sim 19$ mag i.e. near the limit of photographic magnitudes;

(iii) the agreement is satisfactory between the present and other CCD data.

3.1. Compiled catalogue

In order to provide the best $UBVRI$ photometric measurements available for the stars in the region of NGC 7790, we transferred various observations on a common photometric system and prepared a compiled catalogue using the results of photometric comparisons carried out in the last section. For this, photographic measurements have not been considered, as they have larger errors. However, this does not introduce any data incompleteness since almost all of them also have photoelectric and/or CCD measurements. For the compiled catalogue, we considered the present BVI data, Phelps & Janes (1994) U data and Romeo et al. (1989) R data as the reference and converted all other photometric data on these systems taking due care for systematic differences, observed in the last section. As the accuracy of photoelectric and CCD measurements is comparable at a given brightness, all measurements of a star in a passband are given equal weight in determining the mean
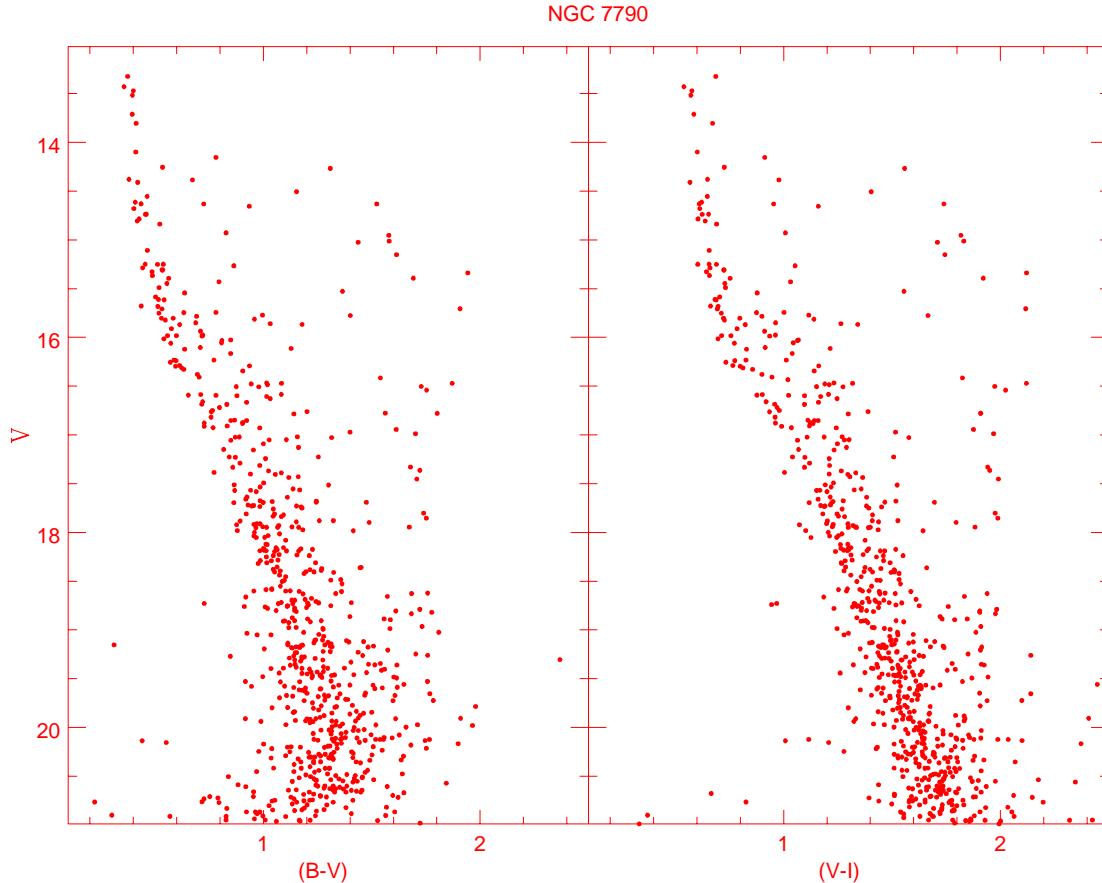
Fig. 2. The $V, (B-V)$ and $V, (V-I)$ diagrams for the stars observed by us in NGC 7790 region

values, in cases, where more than one measurements are available. The compiled catalogue prepared in this way contains U, B, V, R and I measurements for 716, 2099, 2417, 312 and 1315 stars respectively. The stars are spread over an area of $\sim 13' \times 13'$ and have brightness range from $V = 10$ to 22 mag. For brighter stars ($V < 12$), the data are photoelectric only as CCD observations are saturated for them. While for fainter ($V > 15$) stars, the data are mostly from CCD observations.

4. Radius of the cluster

We used radial stellar density profile for the determination of cluster radius which is always a difficult task as

(a) it depends on the limiting magnitude of the members. The more fainter stars one considers, the larger becomes the cluster radius, since such stars occupy larger distances from the cluster center due to two body relaxation;

(b) the level of surrounding field-stars determines the point where the outer or fainter stars merge with the field, so the radius depends on the density of the background;

(c) the number of member stars diminishes with increasing distance from the cluster center, and it becomes hard to detect them in the statistical fluctuations of field-stars.

The radius at which star density flattens in the radial stellar density profile has been considered as cluster radius. This does not correspond either to the core radius or to the tidal radius but it depends mostly on the cluster richness and the field-star density. For determining star density profile, we used the data from DSS as well as from compiled catalogue. From DSS, we extracted an image of size $30' \times 30'$ in 1059×1059 pixel^2 size image frame. Each pixel covers $1''7 \times 1''7$ of the sky which is more than twice the pixel size of the CCD used by us. We adopted the same cluster center as Sandage (1958) did (star E). Figure 4 shows the plot of radial star density profile for both DSS and compiled catalogue data where arrow indicates the cluster radius. Both the data sets yield almost the same value. The cluster radius obtained in this way is $3'.7 \pm 0.2$, which is larger than the value of $2'.5$ given in Lyngå (1987) catalogue. The radial stellar density profile based on DSS data shows that the cluster may not have many members in the coronal region i.e. at radial distance of more than
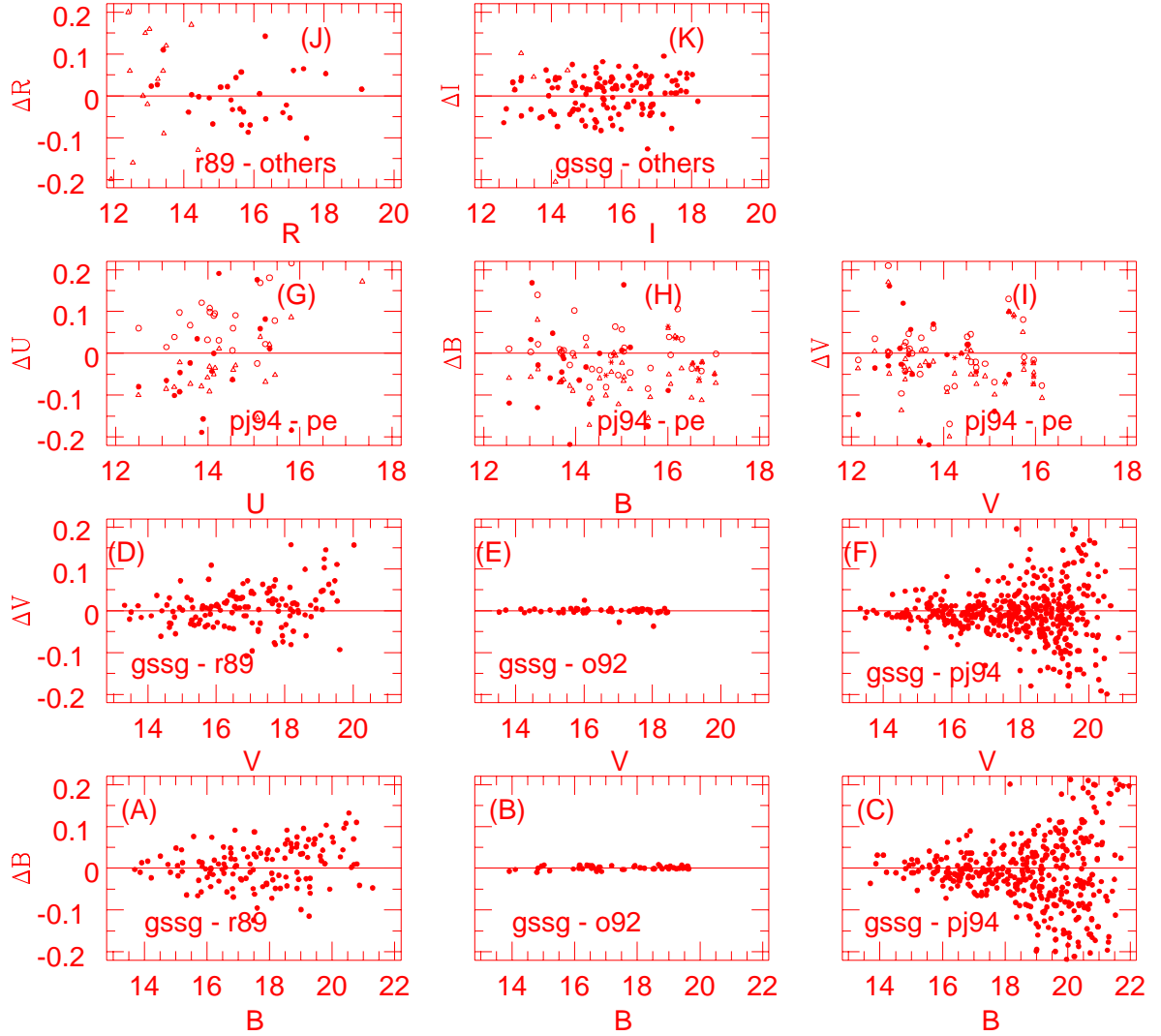
Fig. 3. A comparison of photometric data. The present (gssg) B and V data have been compared with the corresponding CCD magnitudes given by Romeo et al. (1989) (r89), Odewahn et al. (1992) (o92) and Phelps & Janes (1994) (pj94) in **A), B), C), D), E)** and **F)** diagrams. The U, B and V CCD data of pj94 are compared with the corresponding photoelectric data given by Sandage (1958) (open circles); by Alcalá & Ferro (1988) (filled circles); by Turner (1994) (open triangles) and by Christian et al. (1985) (asterisked) in **G), H)** and **I)** diagrams. In **J)** diagram, the R data provided by r89 have been compared with CCD R magnitudes given by Odewahn et al. (1992) (filled circles) and with the photoelectric R magnitudes given by Alcalá & Ferro (1988) (open triangles). Present I data have been compared with the CCD I data given by r89 (filled circles) and with the photoelectric I data given by Alcalá & Ferro (1988) (open triangles) in **K)** diagram

1.5 cluster radius. However, deep proper motion and radial velocity measurements are desired to identify them.

5. Field-star contamination and cluster parameters

In order to maximise the cluster members and reduce field-star contamination in the sample to be used for determination of cluster parameters, we have considered stars within a radius of 200 CCD pixel ($\sim 2\rlap{.}'5$) from the cluster center. In the sample, we have also included the stars identified as proper motion members in the cluster database by

Mermilliod (1995). As these stars are generally bright ($V < 14$ mag), they are very important for the determination of cluster age and for the study of stellar evolutionary status of the Cepheids and other evolved stars. Before deriving cluster parameters from this sample, we shall quantify the amount of field-star contamination and the same is done below.

5.1. Field-star contamination

As the cluster location near the Perseus arm contributes a good number of background and foreground stars,

Table 3. Statistical results of the photometric comparison are presented here. The mean and standard deviation (σ) of the differences (Δ) are based on N stars given inside bracket. Photoelectric and photographic data given by Sandage (1958) are denoted by s58pe and s58pg respectively. Alcalá & Ferro (1988); Frolov (1977); Christian et al. (1985); Turner (1994); Pedreros et al. (1984); Odewahn et al. (1992); Phelps & Janes (1994) and Romeo et al. (1989) have been abbreviated as a88pe, f77pg, c85pe, t94pe, p84pg, o92ccd, pj94ccd and r89ccd respectively

| Comparison data	V range	ΔU Mean $\pm\sigma(N)$	ΔB Mean $\pm\sigma(N)$	ΔV Mean $\pm\sigma(N)$	ΔI Mean $\pm\sigma(N)$
s58pe−a88pe	11.0 − 15.3	$-0.05 \pm 0.10(10)$	$-0.04 \pm 0.05(11)$	$-0.01 \pm 0.05(11)$	
s58pe−t94pe	11.0 − 15.3	$-0.12 \pm 0.04(22)$	$-0.07 \pm 0.02(33)$	$-0.03 \pm 0.02(33)$	
pj94ccd−s58pe	12.0 − 15.6	$0.07 \pm 0.06(22)$	$-0.01 \pm 0.04(30)$	$-0.01 \pm 0.05(30)$	
pj94ccd−c85pe	12.0 − 15.3		$-0.02 \pm 0.04(10)$	$-0.01 \pm 0.06(10)$	
pj94ccd−a88pe	12.0 − 15.3	$-0.03 \pm 0.13(22)$	$-0.05 \pm 0.10(22)$	$-0.01 \pm 0.12(22)$	
pj94ccd−t98pe	12.0 − 15.3	$-0.04 \pm 0.07(23)$	$-0.05 \pm 0.05(41)$	$-0.03 \pm 0.07(41)$	
Present−s58pe	13.5 − 15.8		$0.01 \pm 0.04(11)$	$-0.01 \pm 0.06(11)$	
Present−a88pe	13.3 − 15.5		$-0.07 \pm 0.07(10)$	$-0.01 \pm 0.10(9)$	
Present−s58pg	13.3 − 16.1		$0.04 \pm 0.07(52)$	$0.04 \pm 0.05(52)$	
Present−f77pg	13.3 − 14.0		$-0.02 \pm 0.03(4)$	$0.06 \pm 0.02(4)$	
	14.0 − 15.0		$0.05 \pm 0.07(9)$	$0.03 \pm 0.06(9)$	
	15.0 − 15.8		$0.07 \pm 0.05(10)$	$-0.02 \pm 0.05(10)$	
Present−p84pg	13.3 − 15.0		$0.01 \pm 0.05(15)$	$0.07 \pm 0.06(15)$	
	15.0 − 17.0		$0.02 \pm 0.05(63)$	$0.09 \pm 0.06(63)$	
	17.0 − 19.6		$0.23 \pm 0.06(60)$	$0.20 \pm 0.08(60)$	
Present−r89ccd	13.3 − 15.0		$0.00 \pm 0.02(18)$	$0.02 \pm 0.03(18)$	$-0.03 \pm 0.04(19)$
	15.0 − 17.0		$-0.01 \pm 0.03(44)$	$0.01 \pm 0.04(44)$	$-0.04 \pm 0.04(45)$
	17.0 − 19.5		$0.05 \pm 0.07(41)$	$0.03 \pm 0.06(41)$	$-0.04 \pm 0.05(43)$
Present−o92ccd	13.5 − 15.0		$0.01 \pm 0.03(7)$	$0.03 \pm 0.04(7)$	
	15.0 − 17.0		$-0.03 \pm 0.02(22)$	$-0.02 \pm 0.03(22)$	
	17.0 − 18.5		$-0.02 \pm 0.07(20)$	$-0.07 \pm 0.08(20)$	
Present−pj94ccd	13.5 − 15.0		$0.00 \pm 0.02(27)$	$0.03 \pm 0.01(27)$	
	15.0 − 17.0		$0.03 \pm 0.01(111)$	$0.03 \pm 0.03(111)$	
	17.0 − 20.0		$0.08 \pm 0.09(240)$	$0.06 \pm 0.08(296)$	
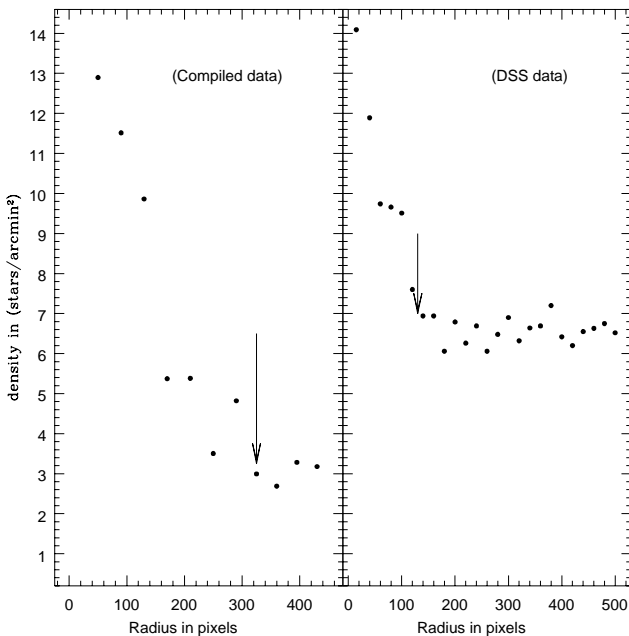
Fig. 4. Plot of radial stellar density profiles determined from the compiled catalogue and DSS data having a pixel of size $0\rlap{.}''74$ and $1\rlap{.}''7$ respectively. Arrows denote the radius where the stellar density seems to merge with the field-star density

it is difficult to separate the field-stars from the cluster members, only on the basis of their closeness to the MS in the CMD and colour-colour diagrams of the cluster (see Romeo et al. 1989, for a detailed discussion). The probability of cluster membership is small for stars located well away from the MS. To know the actual number of cluster members from the remaining stars, their kinematic information like proper motions and radial velocities are required. Due to lack of such information for stars fainter than $V \sim 13$ mag, it is difficult to establish firmly the cluster membership of these stars. In order to get an idea of the field-star contamination in the cluster region, Pedreros et al. (1984) measured stars in the adjacent field (see their Fig. 1) which is located at $\sim 8'$ (i.e about ~ 2.2 cluster radius) away from the cluster center. So, we also consider it as the field region. Frequency distribution of the stars in different parts of the V, $B-V$ diagram in the cluster and field regions normalized for the difference in their areas is listed in Table 4. In order to avoid the effect of relatively large data incompleteness, the analysis is restricted to the brightness level which is ~ 1 mag above the limiting magnitude of Pedreros et al. (1984) observations. To derive the frequency distribution of stars, the V, $(B-V)$ diagram is divided into seven magnitude bins from $V = 12$ to 19 and three colour bins called *blueward,*

Table 4. Frequency distribution in the $V, (B - V)$ diagrams of the cluster region and adjacent field region (taken from Pedreros et al. 1984) are presented. The number of stars in the cluster and field regions are normalised to the cluster area. N_{BC}, N_{MC} and N_{RC} denote the number of stars in the cluster region located blueward, near and redward of MS respectively. The corresponding numbers for the field region are N_{BF}, N_{MF} and N_{RF} respectively

V	N_{BC}	N_{BF}	N_{MC}	N_{MF}	N_{RC}	N_{RF}
12.0−13.0	0	0	4	4	1	4
13.0−14.0	0	0	13	0	4	11
14.0−15.0	0	0	14	0	12	7
15.0−16.0	0	0	39	4	17	14
16.0−17.0	0	0	63	25	38	21
17.0−18.0	5	18	75	39	32	21
18.0−19.0	16	18	117	32	35	25

near and *redward* of MS. We find that the number of MS stars is generally more than that in adjacent field area and that the differences are statistically significant, while the differences in the numbers of stars, which are blueward of MS and redward of MS, of the two regions are generally not statistically significant. The table indicates that the degree of field-star contamination in the MS of our sample is increasing with faintness. The cluster parameters are derived using the sample stars assuming that field-star contamination may not change the results derived below significantly.

5.2. Interstellar extinction in the direction of cluster

In order to estimate the interstellar extinction to the cluster, we plot apparent $(U - B)$ versus $(B - V)$ diagram in Fig. 5 for the sample stars. Adopting the slope of reddening line $E(U - B)/E(B - V)$ as 0.72, we fitted the intrinsic zero−age main−sequence (ZAMS) given by Schmidt-Kaler (1982) to the MS stars of spectral type earlier than A0 in Fig. 5. This yields a mean value of $E(B - V) = 0.51$ mag with an uncertainty of ~ 0.03 mag for NGC 7790. The observed cluster sequence in Fig. 5 is well defined for hotter stars, indicating that interstellar extinction is uniform across the cluster region in agreement with the conclusions made by Sandage (1958); Pedreros et al. (1984) and Romeo et al. (1989). Our reddening estimate agrees fairly well with most of the earlier estimates (see Table 2 in Romeo et al. 1989), except in the case of the photographic determination of Pedreros et al. (1984) which has a value of 0.64 ± 0.04 mag.

For determining the nature of interstellar extinction law in the direction of the cluster, we used the stars earlier than A0 selected from their location in the $(U - B)$ versus $(B - V)$ diagram (Fig. 5) which reveals that stars with $(B - V) < 0.65$ mag are the desired objects. For them, the $(B - V)_0$, $E(B - V)$ and $E(U - B)$ values have been determined using the spectral type
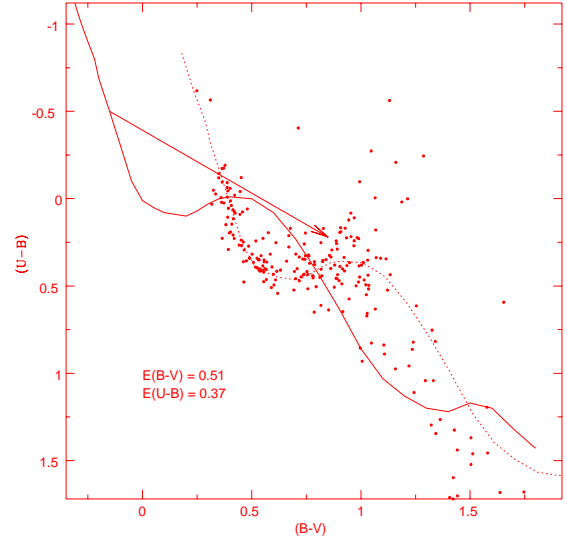

Fig. 5. The $(U - B), (B - V)$ diagram for the sample stars in NGC 7790. The continuous straight line represents the slope (0.72) and direction of the reddening vector. The dotted curve represents the locus of Schmidt−Kaler's (1982) ZAMS, shifted in the direction of reddening vector for the values of $E(B - V)$ and $E(U - B)$ indicated in the diagram

(available only for 10 stars) taken from the cluster database and the UBV photometric Q method (cf. Johnson & Morgan 1953; Sagar & Joshi 1979), and the calibration given by Schmidt-Kaler (1982). For calculating $E(V - R)$ and $E(V - I)$ values, we used the apparent $(V - R)$ and $(V - I)$ measurements; Sagar & Cannon's (1994) calibration between $(B - V)_0$ and $(V - R)_0$ and Walker's (1985) calibration between $(B - V)_0$ and $(V - I)_0$. The mean values of the colour-excess ratios derived in this way are listed in Table 5. They are in fair agreement with the normal values. We have therefore considered normal and uniform interstellar extinction in the direction of the cluster with $E(B - V) = 0.51$ mag in our further analyses.

5.3. The CMDs and distance to the cluster

In order to determine the distance modulus of the cluster, we plot intrinsic $V_0, (U - V)_0$; $V_0, (B - V)_0$; $V_0, (V - R)_0$ and $V_0, (V - I)_0$ diagrams in Fig. 6 for the sample stars of NGC 7790. For this, we convert apparent V magnitude and $(B - V), (U - B), (V - R)$ and $(V - I)$ colours into intrinsic ones using the value of $E(B - V) = 0.51$ mag and following relations for $E(U - B); E(V - R); A_v$ and $E(V - I)$ (see Sagar & Cannon 1994 and references therein)

$$\frac{E(U - B)}{E(B - V)} = X + 0.05E(B - V)$$

Table 5. A comparison of the colour-excess ratios with $E(B-V)$ for NGC 7790 with the corresponding values for the normal interstellar extinction law given by Schmidt-Kaler (1982) for $E(U-B)/E(B-V)$; by Alcalá & Ferro (1988) for $E(V-R)/E(B-V)$ and by Dean et al. (1978) for $E(V-I)/E(B-V)$

Object	$E(B-V)$	$E(U-B)/E(B-V)$	$E(V-R)/E(B-V)$	$E(V-I)/E(B-V)$
Normal interstellar		0.72	0.65	1.25
NGC 7790 (spectroscopic)	0.51 ± 0.04	0.71 ± 0.04	0.65 ± 0.04	1.32 ± 0.05
NGC 7790 (photometric)	0.51 ± 0.06	0.69 ± 0.05	0.66 ± 0.05	1.38 ± 0.07

where $X = 0.62 - 0.3(B-V)_0$ for $(B-V)_0 < -0.09$
and $X = 0.66 + 0.08(B-V)_0$ for $(B-V)_0 > -0.09$;

$$\frac{E(V-R)}{E(B-V)} = E1 + E2 \times E(B-V)$$

where $E1 = 0.6316 + 0.0713(B-V)_0$ and
$E2 = 0.0362 + 0.0078(B-V)_0$;

$$\frac{A_v}{E(B-V)} = 3.06 + 0.25(B-V)_0 + 0.05E(B-V)$$

and

$$\frac{E(V-I)}{E(B-V)} = 1.25[1 + 0.06(B-V)_0 + 0.014E(B-V)].$$

As the interstellar extinction seems to be uniform across the cluster region (see last section), we have used the same value of $E(B-V)$ for all sample stars.

The overall morphology of the CMDs confirms those obtained by earlier studies (Sandage 1958; Pedreros et al. 1984; Romeo et al. 1989; Phelps & Janes 1994). In all the CMDs a well populated cluster MS down to $V_0 = 18$ mag is clearly seen. The $V_0, (B-V)_0$ and $V_0, (V-I)_0$ diagrams show the faintest part of the MS. Evolutionary effects are clearly visible in the upper part of the cluster MS. The stars seem to be distributed in a clumpy fashion along the MS, giving rise to gaps. The most prominent one amongst them is located near turn-off point (see Fig. 6). It has a width of ~ 0.25 mag. Following Hawarden (1971), the χ^2 value of this gap is estimated and found to be 0.012% indicating that this is a genuine gap. This gap is similar to the those observed on the rising branches of the evolving part of MS (cf. Sagar & Joshi 1978 and references therein).

In $V_0, (U-V)_0$ and $V_0, (B-V)_0$ diagrams, we fitted the ZAMS given by Schmidt-Kaler (1982) while in $V_0, (V-R)_0$ and $V_0, (V-I)_0$ diagrams, the ZAMS given by Walker (1985) was fitted. The $(V-R)_0$ colour for the ZAMS on the present photometric system was taken from Sagar & Cannon (1994). After accounting for the colour dispersion expected from the error in observations, the visual fit of the ZAMS to the bluest envelope of the CM diagrams gives $(m-M)_0 = 12.6 \pm 0.1$. The visual fit has been done for stars in the unevolved part of the MS ($V_0 > 14$ mag).

The mean value of $(m-M)_0$ is 12.6 ± 0.15 mag for NGC 7790. The uncertainty in the value is estimated from the errors in $R, E(B-V)$ and the errors in fitting the ZAMS. The distance modulus yields a distance of 3300 ± 230 pc to NGC 7790. Present determination

of distance modulus agrees with those recently determined by Romeo et al. (1989) and Phelps & Janes (1994). However, it is larger than the values of 12.3, 12.15 and 11.98 mag determined by Pedreros et al. (1984), Balona & Shobbrook (1985) and Schmidt (1981) respectively. Present distance determination should be considered as more reliable because they have been derived by fitting the ZAMS over a wide range of the unevolved part of the cluster MS.

As the cluster contains three Cepheid variables, we have used the period-luminosity relation (PLR) given by Sandage et al. (1999) for the Galactic Cepheids for determining their distance modulus. For this, the average $<V>$ values and observed period given in Table 6 are used. This yields a value of 12.63 ± 0.1 mag for the true distance modulus of the Cepheids assuming present detemination of $E(B-V)$ and the value of R given above. Thus, the agreement between two independent estimates of distance is excellent. The present distance determination also agrees very well with the value of 3230 ± 160 pc determined for the Cepheid CF Cas by Matthews et al. (1995) using the PLR.

5.4. Age of the cluster members

The stars brighter than $M_v = 0.0$ mag show evolutionary effects and most of them are proper motion cluster members. In order to derive the cluster age, we converted apparent $V, (B-V)$ diagram of the sample stars into intrinsic ones. We used this diagram instead of other CMDs as the other colours are not available for all bright stars. Figure 7 shows the $M_v, (B-V)_0$ diagram for NGC 7790. We have estimated age by fitting stellar evolutionary isochrones given by Bertelli et al. (1994) in Fig. 7. The isochrones include the effects of mass loss and overshooting of the convective core in the theoretical calculations. The effects of the binaries have also been considered while estimating ages. In order to define upper limit of the effects of binarity in the CMDs, the isochrones which are derived from theoretical stellar evolutionary models for single stars have been brightened by 0.75 mag keeping the colour same. The isochrones fitted in this way explains the presence of stars around the MS and the red GB. This also indicates that some fraction of cluster members seems to be in the form of binaries. The population I ($X = 0.7, Y = 0.28, Z = 0.02$) isochrone of age $\log t = 8.1$ fits the brighter
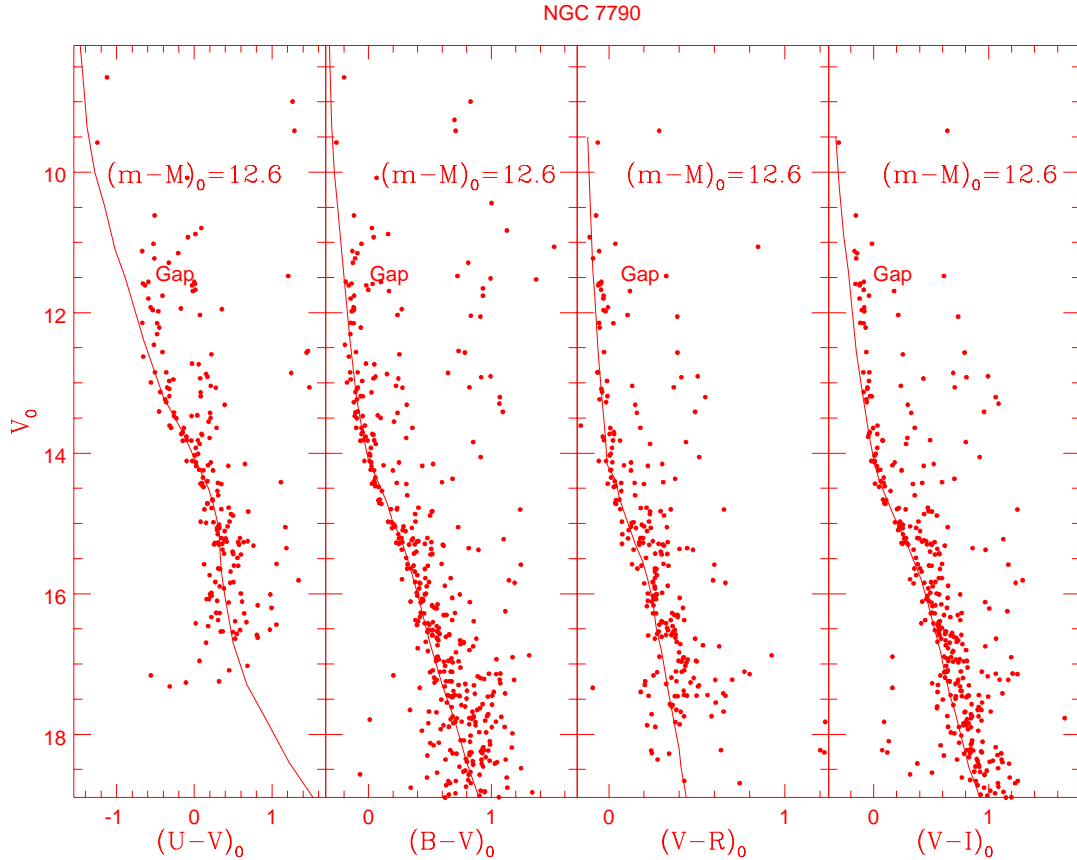
Fig. 6. The V_0, $(U-V)_0$; V_0, $(B-V)_0$; V_0, $(V-R)_0$ and V_0, $(V-I)_0$ diagrams for the sample stars in NGC 7790. Continuous curves are the ZAMS fitted to the unevolved part of the cluster MS for the values indicated in the diagram. The mean value of true distance modulus $(m-M)_0$ to the cluster is 12.6 mag

MS stars, except the two bluest and brightest stars (see Fig. 7). As they are located near ZAMS in the CMDs (see Fig. 6) and also have high probability of proper motion cluster membership, we consider them as blue straggler as Ahumada & Lapasset (1995) did.

The positions of the Cepheid variables CEa Cas, CEb Cas and CF Cas are shown as crosses in Fig. 7. For this, we used the photometric data provided by Sandage (1958) for CF Cas and by Opal et al. (1987) for others. The extremes of their variabilty are also indicated. For the Cepheids, the blue loop of the solar metallicity isochrones does not reach the instability strip, which was also noticed by Romeo et al. (1989). At the same time, their spectroscopic chemical abundance determinations indicate lower metallicity of [Fe/H] = −0.2 (Fry & Carney 1997). In order to see whether the lower metallicity isochrones fit these variables, we fit the $Z = 0.008$ isochrones given by Bertelli et al. (1994). The single star isochrone fits the Cepheid variables well for an age of log t = 8.1 but for slightly different cluster parameters which can be accounted in terms of the colour difference expected at different chemical composition. This, therefore supports the lower metallicity determination of the Cepheids by Fry

& Carney (1997) and also the fact that the Cepheids are known to be single stars. However, their observed positions (more or less in the middle of the blue loop) are not at the generally expected location which is near the bluest point of the blue loop, where the life time is relatively longer. This may indicate that either theoretical loop morphology is not completely correct as it depends on several variables (main being the mass loss rate and metallicity) of the Cepheids which are not accounted in the model or they are in extremely fast evolutionary stage with the brightest one passed the bluest point while other two are approaching towards it.

In the light of the above discussions, we conclude that the cluster is 120 ± 20 Myr old. This agrees very well with the value of 100 Myr given by Romeo et al. (1989).

6. The Cepheids as distance calibrators

Cepheids variables are the principal distance indicators upon which the calibration of the extragalactic distance scale currently rests, and one of the most nagging contributors to uncertainty in that scale is the Galactic Cepheid calibration (see Feast & Walker 1987
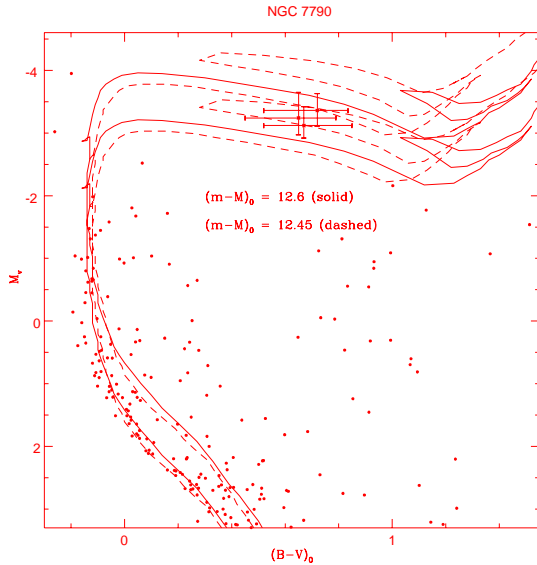
Fig. 7. The $M_v, (B-V)_0$ diagram of NGC 7790. It is plotted only for brighter stars ($(B-V)_0 < 1.5$ mag and $M_v < 3.4$ mag) so that various type of stars can be identified clearly. The two stars located above and blueward of the cluster turn-off point are blue stragglers. The three Cepheid variables have been shown with crosses denoting extremes of their variability. Isochrones of age $\log t = 8.1$ from Bertelli et al. (1994) for both Pop. I (solid) and $Z = 0.008$ (dashed) have been fitted to the bright cluster members and the MS for the marked values of distances. The extent of brightening in the corresponding isochrones due to binaries of equal mass are also shown. An age of ~ 120 Myr is thus assigned to NGC 7790

Table 6. Mean $<V>$ mag and Period P in days for the Cepheids in NGC 7790 are taken from Sandage (1958) and Opal et al. (1987). The $<M_v>$ values are derived assuming Cepheids as cluster member and using present determination of distance and reddening. The zero-points ($C1$) are determined using these $<M_v>$ in the period-luminosity relation given by Sandage et al. (1999)

Cepheid	P	$<V>$	$<M_v>$	$C1$
	(day)	(mag)	(mag)	(mag)
CEa Cas	5.14087	10.90	-3.36	-1.35
CEb Cas	4.47928	11.02	-3.24	-1.40
CF Cas	4.87522	11.14	-3.12	-1.18
Average				-1.31 ± 0.1

for a review). Using all the available photometric and spectroscopic data, we have determined the reliable reddening as well as distance values to the cluster. They can therefore be used to refine the zero-point of the extragalactic distance scale, since three Cepheids are members of this cluster. Sandage et al. (1999) have shown that the PLR is $<M_v> = -2.82 \log P + C1$; where $C1$ is the zero-point and it needs to be determined precisely. The periods and average $<V>$ magnitudes of the Cepheids present in this cluster are listed in Table 6. These $<V>$ magnitudes and the present determination

of distance and reddening to the NGC 7790 are used to determine their $<M_v>$ values (see Table 6). These along with the periods used in the PLR, allow to determine the values of $C1$ for all Cepheids as indicated in Table 6. The average value (-1.31 ± 0.1) of $C1$ agrees very well with the value of -1.34 given by Sandage et al. (1999) using theoretical models for solar metallicity. However, a lower metallicity for the NGC 7790 Cepheids will not change the value as according to Sandage et al. (1999) the luminosity dependence on metallicity is very week ($\frac{dM_v}{d[\text{Fe/H}]} = -0.081$).

Periods of the Cepheids can also be used to determine their ages. Romeo et al. (1989) estimated an age of 120 Myr for the Cepheids of NGC 7790 using the period-age relation derived from those stellar evolutionary models where convective core overshooting and mass loss are taken into account. Thus the age of the Cepheids is consistent with the age of the cluster derived by fitting of isochrones in the $M_v, (B-V)_0$ diagram (see Fig. 7).

7. Discussions and conclusions

Using all available photoelectric and CCD multi-colour $UBVRI$ photometric data including the present deep CCD BVI photometry, the best set of magnitudes and colours are calculated for the stars of NGC 7790 region. In the absence of kinematical data for most of stars fainter than $V \sim 13$, it is difficult to separate unambiguously cluster members from the field-stars only on the basis of available photometric observations. The radial stellar density profile indicates that the cluster radius is $3'.7 \pm 0.2$. Using stars located well within a cluster radius, we determine the most reliable values of $E(B-V)$ and the true distance modulus as 0.51 ± 0.03 and 12.6 ± 0.15 mag respectively. This value of distance agrees very well with that determined from Cepheids using the PLR given by Sandage et al. (1999). The interstellar reddening across the cluster region is uniform and normal.

The cluster contains a well defined MS with a gap on the evolving part of the MS. It also contains two blue stragglers, a few bright red giants and three Cepheids, all having proper motion membership. The upper MS of the cluster shows evolutionary effects. The spectroscopic data of a few stars on the brighter part of the MS indicate that they are of B spectral type and of IV luminosity class. Their location in the $M_v, (B-V)_0$ diagram also indicates that they are in the sub-giant phase of stars, just evolving off the MS. Both the bright MS stars and the Cepheid variables are fitted well with the $Z = 0.008$ metallicity isochrone, rather than the solar metallicity isochrones. An age of 120 ± 20 Myr has been derived in this way for the NGC 7790.

Both age and distance estimates for the Cepheid variables are consistent with the present determination

of reddening, distance and age to the cluster NGC 7790. This supports the cluster membership of the Cepheids.

References

Ahumada J., Lapasset E., 1995, A&AS 109, 375

Alcalá J.M., Ferro A.A., 1988, Rev. Mex. Astro. Astrofis. 16, 81

Balona L.A., Shobbrook R.R., 1985, Cepheids: Theory and Observations, IAU Coll. 82, Madore B.F. (ed.). Cambridge University Press, p. 201

Bertelli G., Bressan A., Chiosi C., Fagotto F., Nasi E., 1994, A&AS 106, 275

Christian C.A., Adams M., Barnes J.V, Butcher H., Hayes D.S., Mould J.R., Sieegel M., 1985, PASP 97, 363

Dean F.J., Warren P.R., Cousins A.W.J., 1978, MNRAS 183, 569

Feast M.W., Walker A.R., 1987, ARA&A 25, 345

Frolov V.N., 1977, Izv. Glavn. Astr. Obs. Pulkove 195, 80

Fry A.M., Carney B.W., 1997, AJ 113, 1073

Hawarden T.G., 1971, The Observatory 91, 78

Ishmukamedov K., 1966, Circ. Tashkent Astr. Obs. 345

Iyeshima T., Okyudo M., Sadakane K., 1994, Ann. Rep. Nishi - Harima Astron. Obs. 4, 18

Johnson H.L., Morgan W.W., 1953, ApJ 117, 313

Kraft R.P., 1958, ApJ 128, 161

Landolt A.V., 1983, AJ 88, 439

Lyngå G., 1987, Catalogue of open cluster data, 5th edition, 1/1 S7041, Centre de Données Stellaires, Strasbourg

Matthews J.M., Gieren W.P., Mermilliod J.C., Welch D.L., 1995, AJ 110, 2280

Mermilliod J.C., 1981, A&AS 97, 235

Mermilliod J.C., 1995, in Information and on − line data in Astronomy, Egret E., Abrecht M.A. (eds.). Kluwer Academic Press, p. 227

Odewahn S.C., Bryja C., Humphreys R.M., 1992, PASP 104, 553

Opal C.B., Krist J.E., Barnes T.G., Moffett T.J., 1987, BAAS 19, 1052

Pedreros M., Madore B.F., Freedman W.L., 1984, ApJ 286, 563

Phelps R.L., Janes K.A., 1994, ApJS 90, 31

Romeo G., Bonifazi A., Fusi Pecci F., Tosi M., 1989, MNRAS 240, 459

Sagar R., Cannon, R.D., 1994, BASI 22, 381

Sagar R., Griffiths W.K., 1991, MNRAS 250, 683

Sagar R., Joshi U.C., 1978, BASI 6, 37

Sagar R., Joshi U.C., 1979, Ap&SS 66, 3

Sandage A.R., 1958, ApJ 128, 150

Sandage A., Bell R.A., Tripicco M.J., 1999, ApJ 522, 250

Schmidt E.G., 1981, AJ 86, 242

Schmidt−Kaler Th., 1982, in: Landolt/Bornstein, Numerical Data and Functional Relationship in Science and Technology, New series, Group VI, Vol. 2b, Scaifers K., Voigt H.H. (eds.). Springer-Verlag, Berlin, p. 14

Stetson P.B., 1987, PASP 99, 191

Stetson P.B., 1992, IAU Col. 136 on stellar photometry - current techniques and future developments, Butler C.J., Elliott I. (eds.), p. 291

Turner D., 1994 (private communication)

Walker A.R., 1985, MNRAS 213, 889

Zhao J.L., Tian K.P., Jing J.Y., Yin M.G., 1984, Special Issue for Tables of Membership for 42 open clusters, Shangai